Lithuanian Journal of Physics, Vol. **44**, No. 1, pp. 49–57 (2004)

GRADED-GAP $Al_xGa_{1-x}As$ IONIZING RADIATION DETECTORS *

A. Šilėnas

Semiconductor Physics Institute, A. Goštauto 11, LT-01108 Vilnius, Lithuania
E-mail: silenas@pfi.lt

Received 17 October 2003

Fabrication and measurements of the graded-gap $Al_xGa_{1-x}As$ ionizing radiation detectors are reviewed. Operating principles of the detectors with optical and electric response are discussed. High X-ray light internal conversation efficiency and X-ray image spatial resolution better than 15 lines/mm are obtained for detectors of square area 2×3 cm^2 with optical response. The main factor reducing the external conversation efficiency is high total internal reflection from the surface. Graded-gap electric field enables 100% generated charge collection in $Al_xGa_{1-x}As$ layer of thickness 27 μm without application of any external voltage. Due to this property, the graded-gap p-$Al_xGa_{1-x}As$/n-GaAs structure can be used as a high-efficiency soft X-ray and single particles (^{241}Am alpha particles) detector operating without any bias. The new charge multiplication method, by increasing reverse current, was realized in the p^+-$Al_xGa_{1-x}As$/n-GaAs graded-gap structures, in which the multiplication coefficient exceeded 200.

Keywords: radiation imaging, X-ray detector, graded-gap $Al_xGa_{1-x}As$ structures

PACS: 73.40.Kp, 07.85.–m

1. Introduction

Graded-gap epitaxial $Al_xGa_{1-x}As$ layers and multilayer structures are promising materials for detectors of ionizing radiation. The change of the Al fraction x along the thickness of the layer causes change in the energy band structure which is responsible for specific properties of graded-gap $Al_xGa_{1-x}As$ layer [1]. The energy gap between the conduction and valence band increases from 1.42 to 1.9 eV with increasing x in the interval $0 < x < 0.4$. The most important property of graded-gap structures is a wide-gap optical window for transmission without absorption of the emitted light in the crystal and the presence of an internal graded-gap electric field that can collect generated charge without application of any external voltage. Graded-gap $Al_xGa_{1-x}As$ structures can be used as ionizing radiation detectors operating either in optical or electric response mode.

2. Detectors with optical response

The detection of charge generated by ionizing radiation by using conversion of the charge to recombination infrared light has many advantages compared with detection by direct electric charge collection. The detector with optical response does not need an electric supply nor electric signal preamplifiers. This property permits one to get a high density of the detector integration (there is no need of the pixel array fabrication) what is important for many practical applications. The material of detector is a doped semiconductor of high conductivity, therefore, the problem of preparation of high resistivity and very pure materials disappears. The transmission of signal from the detector to an electronic system that is outside the active radiation area is much better realized when the signal is optical rather than electric [2].

For the fabrication of the X-ray imaging detectors with optical response, graded-gap $Al_xGa_{1-x}As$ layers of 20–100 mm thickness were grown on GaAs substrates by liquid phase epitaxy. The Al fraction x varied from $x = 0.3$ at the substrate to $x = 0$ on the surface of the layer. To have short luminescence lifetime the layers were doped by Zn acceptor with concentration $p_{Zn} \approx 10^{18}$ cm^{-3}. In order to make the structure transparent for light emission through the wide-gap optical window in the interval 1.5–1.8 eV, the $Al_xGa_{1-x}As$ layer was removed from the GaAs substrate by selective etching [1]. Detectors of area 2×3 cm^2 having ho-

* The report presented at the 35th Lithuanian National Physics Conference, 12–14 June 2003, Vilnius, Lithuania.

ISSN 1648-8504

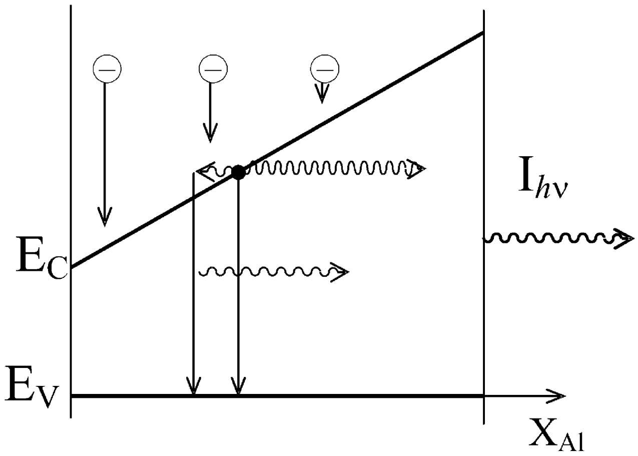

Fig. 1. Schematic view of the band structure of the graded-gap $Al_xGa_{1-x}As$ X-ray detector with optical response.

mogeneous luminescence were fabricated. A shematic band structure of the detector with optical response is shown in Fig. 1.

The calculated dependence of the X-ray absorption coefficient α in the $Al_xGa_{1-x}As$ layer on the photon energy E_X of X-rays shows a large decrease of α with the increase of E_X (see Fig. 2). The $Al_xGa_{1-x}As$ layer of $d = 100$ μm absorbs up to 95% of the X-ray power at energies $E_X < 20$ keV. At $E_X > 50$ keV, the $Al_xGa_{1-x}As$ layer with $d = 100$ μm is transparent to X-rays. Therefore, the $Al_xGa_{1-x}As$ layer of thickness 20–100 μm can be used for detecting soft part of the X-ray spectra with energies less than 30 keV [3].

The experimental measurement of X-ray absorption in $Al_xGa_{1-x}As$ layers was performed using an X-ray tube with a Cu anode. The X-ray intensity spectrum of this source is in the range of $3{\cdot}10^3 < E_X < 3{\cdot}10^4$ eV at the anode voltage of 30 kV with maximum amplitude at $E_X \approx 8$ keV [4]. The measured X-ray absorption coefficient α in this range of E_X is shown in Fig. 2.

The optical image of X-ray intensity was detected by a charge-coupled-device (CCD) camera, and the data were read by a personal computer (PC), Fig. 3. Several other methods of optical response detection with a fibre line or a mirror system can be used. A Si photodiode or a CCD camera can serve as an optical signal receiver.

The efficiency α_c of the conversion of X-ray power absorbed in $Al_xGa_{1-x}As$ to the emitted light power is equal

$$\alpha_c = \beta\eta, \tag{1}$$

where β is the efficiency of the generation of recombined electron–hole (e–h) pairs and η is the part of e–h pairs that recombined with the radiation.

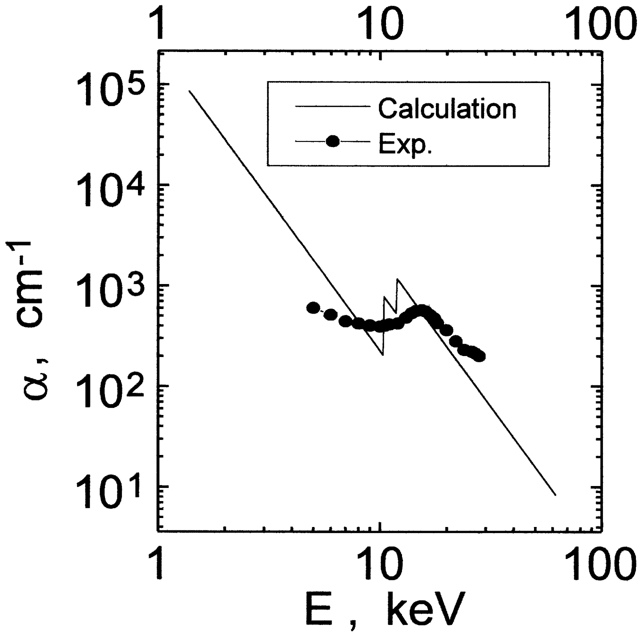

Fig. 2. The X-ray absorption coefficient α in the graded-gap $Al_xGa_{1-x}As$ layer at $x = 0.2$ as a function of X-ray energy E_X. Points represent the experimental data.

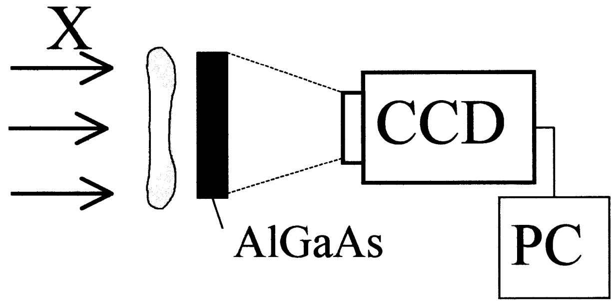

Fig. 3. Set-up for the $Al_xGa_{1-x}As$ X-ray imaging detector.

The generation efficiency of the recombined e–h pairs is determined by the ratio of the emitted photon energy $E_{h\nu}$ and the X-ray threshold energy E_{th}, which is required for the generation of a single e–h pair:

$$\beta = \frac{E_{h\nu}}{E_{th}}. \tag{2}$$

In conventional scintillators and X-ray luminescence screens, $E_{th} = 20-200$ eV and $\beta \approx 1-10\%$, when X-ray power is converted to visible light of energy $E_{h\nu} \approx 2$ eV. Due to low β, the conventional X-ray luminescence screen has low brightness [5]. In $Al_xGa_{1-x}As$ semiconductor material, $E_{th} = 4$ eV, and emitted light energy is $E_{h\nu} \approx 1.6$ eV. In this case, the efficiency is $\beta \approx 40\%$. This is a better performance than of the conventional X-ray–light converters [4].

The efficiency of radiative recombination is equal to

$$\eta = \frac{1}{1 + \tau_\mathrm{r}/\tau_\mathrm{nr}}, \qquad (3)$$

where τ_r and τ_nr are the radiative and nonradiative recombination lifetimes, respectively. The $\mathrm{Al}_x\mathrm{Ga}_{1-x}\mathrm{As}$ layer was doped by Zn acceptors up to the concentration $p_\mathrm{Zn} > 10^{18}$ cm^{-3}. It allows us to reduce $\tau_\mathrm{r} < 10^{-9}$ s at $\tau_\mathrm{nr} = 10^{-9}$ s and to obtain the efficiency of $\eta \approx 0.5{-}0.8$ in our $\mathrm{Al}_x\mathrm{Ga}_{1-x}\mathrm{As}$ detectors. The measurements of the quantum efficiency $\alpha_\mathrm{c} = \beta\eta$ of conversion of the absorbed X-ray power to light beam inside the $\mathrm{Al}_x\mathrm{Ga}_{1-x}\mathrm{As}$ layer show that $\alpha_\mathrm{c} \approx 20\%$, and it is better than in conventional X-ray luminophors or scintillators. The high efficiency α_c allows us to obtain higher signal-to-noise ratio in $\mathrm{Al}_x\mathrm{Ga}_{1-x}\mathrm{As}$ detectors compared with conventional ones.

The external efficiency of X-ray–light conversion of the $\mathrm{Al}_x\mathrm{Ga}_{1-x}\mathrm{As}$ detector is equal to

$$K_\mathrm{ef} = \frac{E_{h\nu}}{E_{\mathrm{X}_0}}, \qquad (4)$$

where $E_{h\nu}$ is the energy of light emitted by the detector and E_{X_0} is the energy of X-ray incident on the detector surface. K_ef is determined by a_X, the part of the X-ray photon energy absorbed in the $\mathrm{Al}_x\mathrm{Ga}_{1-x}\mathrm{As}$ layer, quantum efficiency α_c (see Eq. (1)), and the efficiency γ of light output from the graded-gap $\mathrm{Al}_x\mathrm{Ga}_{1-x}\mathrm{As}$ structure:

$$K_\mathrm{ef} = a_X \alpha_\mathrm{c} \gamma. \qquad (5)$$

For soft X-rays ($E_{\mathrm{X}_0} < 20$ keV) and the $\mathrm{Al}_x\mathrm{Ga}_{1-x}\mathrm{As}$ layer of the thickness ≈ 100 μm one has $a_\mathrm{X} \approx 1$.

The output coefficient γ is equal to

$$\gamma = \frac{TF}{1 - (1 - T)\eta/2}, \qquad (6)$$

where $T = 4n(1 + n)^{-2}$ is the transparency, $F = \sin^2(\theta/2)$ is the factor of total internal reflection, and $\theta = \arcsin n^{-1}$. For the light output from GaAs to air: $n = 3.54$, $T = 0.69$, $\theta = 16°$, $F \approx 2\%$. The factor F reduces the conversion efficiency K_ef most strongly.

Figure 4 shows emitted light measured at energy $E_{h\nu}$ (in CCD camera arbitrary units) as a function of the X-ray exposure time t_exp. The X-ray intensity used was constant, $W_{\mathrm{X}_0} = 5.3 \cdot 10^{-5}$ W/cm^2, and the X-ray energy E_{X_0} absorbed in the $\mathrm{Al}_x\mathrm{Ga}_{1-x}\mathrm{As}$ layer was proportional to the exposure time: $E_{X_0} = 5.3 \cdot 10^{-5}\, t_\mathrm{exp}$ W·s·cm^{-2}.

The experimental results show that the external efficiency of X-ray–light conversion is low ($K \approx 10^{-2}$).

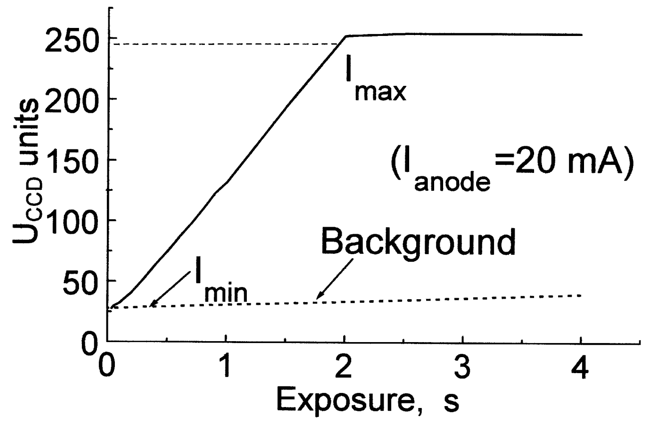

Fig. 4. The X-ray luminescence energy U_CCD in arbitrary units as a function of exposure time. $U_\mathrm{CCD} = 250$ corresponds to the CCD camera saturation level.

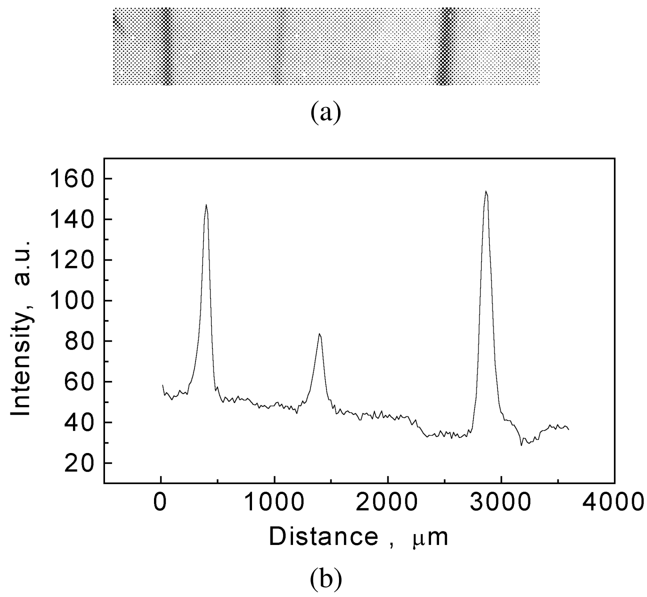

Fig. 5. (a) X-ray luminescence view of three metal wires of thickness 30, 50, 100 μm and (b) luminescence intensity distribution.

The low efficiency $\gamma \approx 10^{-2}$ of the generated light output in the $\mathrm{Al}_x\mathrm{Ga}_{1-x}\mathrm{As}$ layer is responsible for the low level of K_ef. In spite of low K_ef, the large internal efficiency of X-ray–light conversion provides a high signal-to-noise ratio of X-ray luminescence signal.

The experimental determination of the X-ray detector image contrast and spatial resolution shows that the background and noise signals of the used read-out system and CCD camera exceed the fluctuation level of the light emitted from $\mathrm{Al}_x\mathrm{Ga}_{1-x}\mathrm{As}$.

The X-ray luminescence image on the PC monitor and luminescence intensity distribution of three metal wires is shown in Fig. 5. X-ray luminescence image

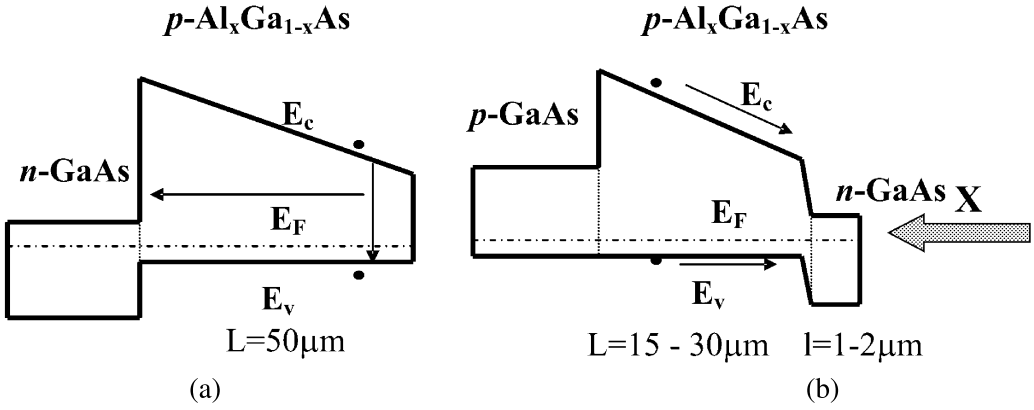

Fig. 6. Schematic band diagrams of (a) n-GaAs/p-$Al_xGa_{1-x}As$ structure with a $p-n$ junction at the wide energy gap side ($x = 0.4$) of the graded-gap layer; (b) p-$Al_xGa_{1-x}As$/n-GaAs structure with a $p-n$ junction at the narrow energy gap side ($x = 0$) of the graded-gap layer.

of different objects obtained by the CCD camera was used for determination of the contrast and spatial image resolution. It is shown that 1.5% luminescence signal variations can be discriminated on the PC monitor. The measurements of the spatial resolution of the $Al_xGa_{1-x}As$ detector were performed using a different type of the masks. It was found that the spatial resolution exceeded 20 lines/mm [3].

The high spatial resolution and contrast allows the $Al_xGa_{1-x}As$ detectors to be used for the X-ray detection of small objects.

3. Detectors with electric response

In spite of a much higher internal quantum efficiency of the X-ray conversion to light the graded-gap $Al_xGa_{1-x}As$ structures, as compared with scintillators, have low external light output efficiency, about a few percent. Consequently, X-ray imaging with the light-emitting $Al_xGa_{1-x}As$ detector needs a long exposure time which can reach up to a few seconds using a charge coupled device (CCD) camera [2].

Two processes are responsible for this low external quantum efficiency of the light-emitting $Al_xGa_{1-x}As$ detector. The first and the main is the strong internal reflection of light excited in the crystal at the $Al_xGa_{1-x}As$/air interface (up to 98%), and the second is the extraction of e–h pairs generated by X-rays from the bulk of the $Al_xGa_{1-x}As$ layer by the internal, graded-gap electric field before their radiative recombination. The second process is important in thin graded-gap structures.

With the aim to eliminate these drawbacks of the light-emitting structures and to increase the X-ray detector sensitivity radically, new nonuniformly doped graded-gap $Al_xGa_{1-x}As$ structures with electric response were proposed and investigated [6].

Two types of graded-gap $Al_xGa_{1-x}As$ structures were investigated:

(1) n-GaAs/p-$Al_xGa_{1-x}As$ structures with a $p-n$ junction at the wide energy gap side ($x = 0.4$) of the graded-gap layer;
(2) p-$Al_xGa_{1-x}As$/n-GaAs structures with a $p-n$ junction at the narrow energy gap side ($x = 0$) of the graded-gap layer.

A graded-gap layer was formed by changing the Al fraction x across the layer thickness L during the epitaxial growth process. The Al fraction varied from $x = 0.4$ at the substrate to $x = 0$ on the surface of the epitaxial graded-gap $Al_xGa_{1-x}As$ layer.

The first type of structures consisted of graded-gap $Al_xGa_{1-x}As$ layers ($L = 50$ μm) grown on an n-GaAs substrate. The graded-gap $Al_xGa_{1-x}As$ layer was doped by Zn up to a hole concentration $p \approx 10^{18}$ cm^{-3}.

The second type of structures was obtained by growing a Zn-doped graded-gap $Al_xGa_{1-x}As$ layer ($L = 15-30$ μm) and an additional thin (1–3 μm) n-GaAs layer on a p-GaAs substrate.

Figure 6 shows schematically the band diagrams of the grown structures. The operating mechanisms of these two types of structure are different depending on the graded-gap $Al_xGa_{1-x}As$ layer thickness. In the structures with a $p-n$ junction at the wide gap side (Fig. 6(a)), X-rays excite luminescence in the graded-gap $Al_xGa_{1-x}As$ layer. This luminescence is transmitted through the wide-gap optical window to the GaAs $p-n$ junction. The $p-n$ junction photovoltaic or current response to the X-ray luminescence was measured. In thin p-$Al_xGa_{1-x}As$/n-GaAs structures with the $p-n$ junction in the narrow gap side (Fig. 6(a)), e–h pairs

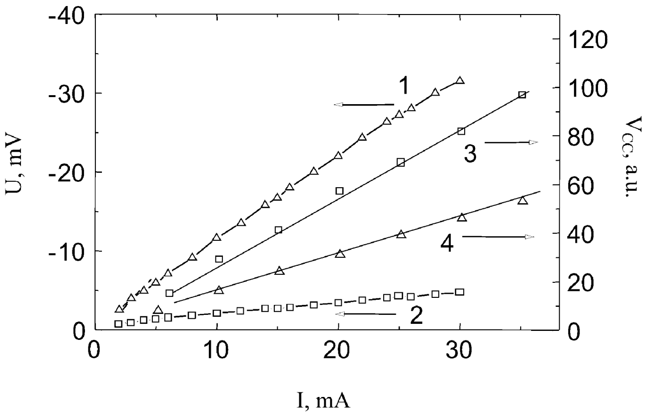

Fig. 7. Voltage response (curves *1,2*) and luminescense intensity (curves *3,4*) dependence on the X-ray tube current for p-Al$_x$Ga$_{1-x}$As/n-GaAs structures with a $p{-}n$ junction at the narrow energy gap side of thickness 15 mum (*1,4*) and 50 μm (*2,3*). X-ray source with a Cr anode was used. Exposure time 1 s for curve *4* and 0.3 s for curve *3*.

generated by X-rays in the graded-gap layer are extracted from the Al$_x$Ga$_{1-x}$As layer and collected at the $p{-}n$ junction by internal graded-gap field before recombination [6, 7]. The influence of internal graded-gap field to charge collection is observed in the experiment shown in Fig. 7. Two structures of different thickness with a potential barrier at the narrow gap side were removed from substrates and X-ray luminescence intensity and voltage response were measured. Photovoltaic response of the thin structure is higher than of the thick one, because of efficient charge collection. However, the luminescence intensity of the thin structure is much lower, because of fast charge extraction from the graded-gap layer. A tube with a Cr anode as a soft X-ray source ($E_{\mathrm{X}} = 5$ keV) was used to attain high absorption efficiency.

The current $j_{\Delta n}$, due to Δn electrons generated in a p-graded-gap Al$_x$Ga$_{1-x}$As layer, is determined by the value of the graded-gap field F_{g}:

$$j_{\Delta n} = e\mu\Delta n F_{\mathrm{g}}, \qquad F_{\mathrm{g}} = \frac{\Delta E_{\mathrm{g}}}{eL}, \tag{7}$$

where ΔE_{g} is the variation of the forbidden energy gap in the Al$_x$Ga$_{1-x}$As layer of thickness L; e and μ are the electron charge and mobility, respectively. This field also determines the carrier collection time, as described below.

Assuming that the generation of e–h pairs in the layer of thickness L is homogeneous, the electron current through the layer can be written as

$$j_{\mathrm{ph}} \approx e\frac{W_{\mathrm{X\ abs}}}{E_{\mathrm{th}}}K, \tag{8}$$

where $W_{\mathrm{X\ abs}}$ is the X-ray power absorbed in the layer, E_{th} is the average energy required for e–h pair generation. $E_{\mathrm{th}} \approx 4$ eV for Al$_x$Ga$_{1-x}$As. The amplification coefficient is

$$K \approx \frac{\tau}{t_{\mathrm{dr}}}, \tag{9}$$

where τ is the e–h pair recombination time and

$$t_{\mathrm{dr}} = \frac{L}{\mu F_{\mathrm{g}}} \tag{10}$$

is the electron drift time through the layer of thickness L.

At $K = 1$ the collection efficiency of generated electrons in the layer of thickness L is 100%. The current-absorbed X-ray power sensitivity of the Al$_x$Ga$_{1-x}$As detector is equal to

$$\beta_j = \frac{j_{\mathrm{ph}}}{W_{\mathrm{X\ abs}}} \approx 0.25K\ [\mathrm{A/W}]. \tag{11}$$

In a thicker layer with lower F_{g}, the electrically collected charge is small because $K \ll 1$. The main part of generated e–h pairs recombines radiatively. The emitted light photons are transmitted to the wide-gap $p{-}n$ junction (see Fig. 6(a)), where they are detected. The detection efficiency in the thick layer is defined mainly by the efficiency of light emission by generated carriers (Eq. (3)).

The voltage response at the junction is equal to

$$U_p = \frac{k_{\mathrm{B}}T}{e}\ln\left(1 + \frac{j_{\mathrm{ph}}}{j_{\mathrm{s}}}\right), \tag{12}$$

where at room temperature $k_{\mathrm{B}}T/e \approx 25$ meV.

Due to the large $\Delta E_{\mathrm{c}} \approx 0.4$ eV, the heterojunction saturation current j_{s} (see Fig. 6(a)) is determined mainly by hole current over the barrier φ_p:

$$j_{\mathrm{s}} \sim p_0 \exp\left(\frac{\varphi_p}{k_{\mathrm{B}}T}\right). \tag{13}$$

Because of large E_{g} in the Al$_x$Ga$_{1-x}$As structure, $\varphi_p/(k_{\mathrm{B}}T) \gg 1$, and $j_{\mathrm{s}} \ll j_{\mathrm{ph}}$ can be expected. Then,

$$U_p = \frac{k_{\mathrm{B}}T}{e}\ln\frac{j_{\mathrm{ph}}}{j_{\mathrm{s}}}. \tag{14}$$

The voltage–absorbed power sensitivity is

$$\beta_v = \beta_j R_p\ [\mathrm{V/W}], \tag{15}$$

where

$$R_p = \frac{U_p}{j_{\mathrm{ph}}}. \tag{16}$$

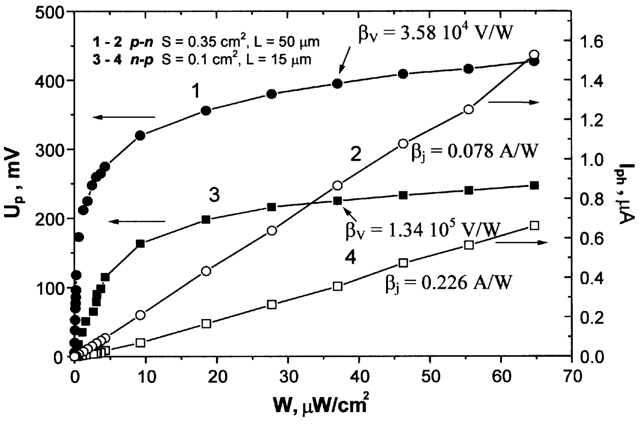

Fig. 8. The current I_{ph} and voltage U_p response dependence on the X-ray power at the surface of the thick ($L = 50$ μm) $Al_xGa_{1-x}As$/GaAs detector with a $p{-}n$ junction at the wide energy gap side (curves *1*, *2*) and the thin ($L = 15$ μm) detector with a $p{-}n$ junction at the narrow energy gap side (curves *3*, *4*).

The resistivity R_p of the junction increases with decrease of $j_{\mathrm{ph}} \sim W_{\mathrm{X\ abs}}$. Consequently, the volt–watt sensitivity

$$\beta_v \sim \frac{\ln W_{\mathrm{X\ abs}}}{W_{\mathrm{X\ abs}}} \tag{17}$$

increases when $W_{\mathrm{X\ abs}}$ decreases.

Figure 8 illustrates the measured dependences of I_{ph} and U_p on the X-ray power W at the surface of the $Al_xGa_{1-x}As$/GaAs detector. One can see that the dependence of the current I_{ph} on the X-ray power $W_{\mathrm{X\ abs}}$ is linear and the dependence of U_p is logarithmic, as predicted by Eqs. (8) and (14). The power absorbed in the detector is

$$W_{\mathrm{X\ abs}} = WSa_x, \tag{18}$$

where S is the detector surface area and a_x is the fraction of the X-rays absorbed in the $Al_xGa_{1-x}As$ layer. For a thick detector with a $p{-}n$ junction, $a_x(50\ \mu m) \approx 0.78$ and $S_{pn} = 0.35$ cm^2. For a thin detector with a $p{-}n$ junction $a_x(15\ \mu m) \approx 0.45$ and $S_{pn} = 0.10$ cm^2. The a_x was estimated from the absorption of X-ray beam with the energy $E_{\mathrm{X}} \approx 8$ keV. In this estimate, the experimental data (Fig. 8) for the ampere–watt sensitivities, $\beta_j = 0.078$ A/W for the thick (50 μm) detector and $\beta_j = 0.226$ A/W for the thin (15 μm) detector, were used. The value of β_j (15 μm) in the thin layer is close to the value 0.25 A/W, predicted by Eq. (11), and corresponds to 100% collection of charge generated in the detector bulk.

The ampere–watt sensitivity of the thin (15 μm) $Al_xGa_{1-x}As$ layer is higher than in the thick (50 μm) one, due to higher charge collection efficiency. But the 15 μm thick $Al_xGa_{1-x}As$ layer is transparent to X-ray photons with energies $E_{\mathrm{X}} \geq 10$ keV.

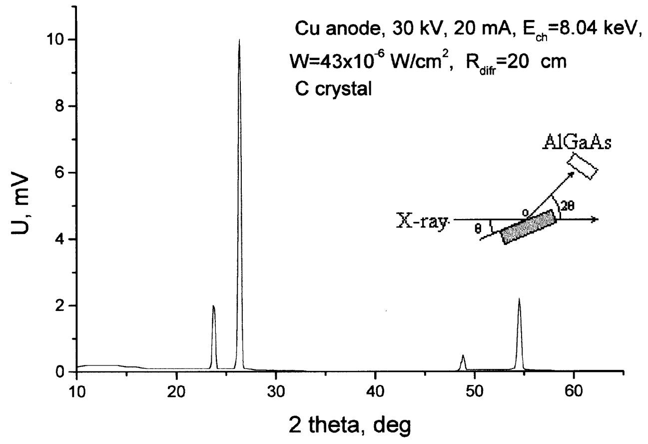

Fig. 9. A diffractogram from a graphite crystal using an X-ray source with a Cu anode. The Cu anode characteristic X-ray photon energy $E_{\mathrm{ch}} = 8.04$ keV is observed.

The observed volt–watt sensitivity, as follows from Eq. (17), is the largest at low absorbed power. At $W_{\mathrm{X\ abs}} \approx 10^{-7}$ W the measured $\beta_v \approx 5{\cdot}10^5$ V/W, and at $W_{\mathrm{X\ abs}} \approx 2{\cdot}10^{-6}$ W it is $\beta_v \approx 1.1{\cdot}10^5$ V/W .

This high volt–watt sensitivity, therefore, allows the use of $Al_xGa_{1-x}As$/GaAs detectors in an X-ray diffractometer instead of the more complex scintillator–photomultiplier arrangement with its associated electronics. Figure 9 demonstrates the diffractogram of a graphite crystal using the X-ray beam from the X-ray source with a Cu anode. One can see that the characteristic line with energy $E_{\mathrm{X}} = 8.04$ keV is very well resolved in this case. Note that the detector noise level is less than 10^{-1} mV.

The fact that the generated carriers are collected without application of any external bias voltage to the detector ensures a low level of noise. Only thermal noise remains as a noise source. This is an important advantage of the $Al_xGa_{1-x}As$/GaAs X-ray and particle detectors compared with $p{-}n$ Si and Schottky barrier diodes which do need a bias voltage and have an additional noise contribution due to leakage current.

4. Detection of single α-particles

A charge generated by a single particle with the energy E_p in an $Al_xGa_{1-x}As$ layer of thickness L is

$$Q_{\mathrm{g}}(L) = q\frac{E_p[1 - \exp\left(-\alpha_p L\right)]}{E_{\mathrm{th}}}, \tag{19}$$

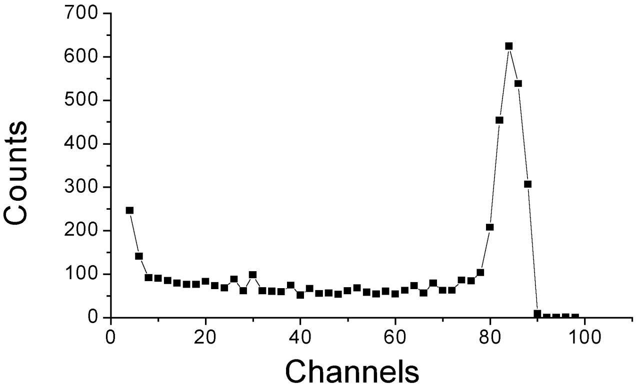

Fig. 10. The energy spectra of alpha particles emitted by ^{241}Am and measured using the graded-gap $Al_xGa_{1-x}As$ detector without any external bias voltage. The thickness of the $Al_xGa_{1-x}As$ layer is $L = 27$ μm.

where q is the electron charge, $E_{\rm th}$ is the threshold energy for generation of a single electron–hole pair, and α_p is the absorption coefficient of particle energy.

The charge drifted in graded-gap field $F_{\rm g}$ from the $Al_xGa_{1-x}As$ layer and collected in the n-GaAs layer is equal

$$Q_{\rm c}(L) = q\frac{E_p}{E_{\rm th}}\frac{\alpha_p[1-\exp{(-\alpha'_pL)}]}{\alpha'}, \quad (20)$$

$$\alpha'_p = \alpha_p + \frac{1}{v_{\rm dr}\tau_{\rm r},} \quad v_{\rm dr} = \mu F_{\rm g}, \quad (21)$$

where μ is the electron mobility and $\tau_{\rm r}$ is the electron–hole recombination time in the $Al_xGa_{1-x}As$ layer.

The collection efficiency of charge generated in the $Al_xGa_{1-x}As$ layer is

$$\eta = \frac{Q_{\rm c}}{Q_{\rm g}}\frac{\alpha_p[1-\exp{(-\alpha'_pL)}]}{\alpha'_p[1-\exp{(-\alpha_pL)}]}. \quad (22)$$

The efficiency η increases with decrease of length L. In thin layers, when $\alpha L < 1$ and $\alpha'_p L < 1$, the efficiency $\eta \approx 1$.

However, the generated charge in the layer decreases when L decreases. The collected charge, which depends on the incident radiation with the energy E_p, is then equal to

$$Q_{\rm X\ inc} = \frac{q}{E_{\rm th}}\eta_{\rm inc}E_p, \quad (23)$$

where

$$\eta_{\rm inc} = \eta\left[1-\exp{(-\alpha_pL)}\right]. \quad (24)$$

The absorption coefficient of 5 MeV alpha particles emitted by ^{241}Am is $\alpha_p \approx 5{\cdot}10^2$ cm^{-1}, and particle penetration depth into GaAs is 23 μm. So, graded-gap $Al_xGa_{1-x}As$ structures of 27 μm thickness were used for alpha particles detection. A 100% generated charge collection without application of any external bias voltage was attained. The measured energy spectra of ^{241}Am alpha particles using the graded-gap $Al_xGa_{1-x}As$ structure are shown in Fig. 10. Since the bias voltage is absent, the noise level is much lower than the amplitude of the collected charge signal [8].

5. Multiplication of collected charge in the n^--GaAs layer

The n^--GaAs/p^+-$Al_xGa_{1-x}As$ structure was prepared for observing the charge multiplication effect. A thin ($l_n < 10^{-4}$ cm) low-doped ($n = 10^{15}$ cm^{-3}) n^--GaAs layer was grown at the narrow-gap side of high-doped ($p = 10^{18}$ cm^{-3}) p^+-$Al_xGa_{1-x}As$ layer ($L = 20$ μm).

In order to multiply the collected charge, the drift time through the thin n^--GaAs layer $t_{\rm dr}(l_n)$ has to be less than the carrier recombination time τ in this layer. The recombination time, experimentally found from the relaxation of photoconductivity in the low-doped n^--GaAs layer, was $\tau \approx 5{\cdot}10^{-6}$ s. It appeared to be much larger than in the high-doped $Al_xGa_{1-x}As$ layer.

To satisfy the condition $t_{\rm dr} \ll \tau$ the reverse voltage is applied to the n^--GaAs/p^+-$Al_xGa_{1-x}As$ heterojunction. At the breakdown of the $p-n$ junction, the increased reverse current I_0 also increases the electric field in n^--GaAs, and as a result, the drift time $t_{\rm dr}$ decreases.

Figure 11 shows the schematic band diagram of the n^--GaAs/p^+-$Al_xGa_{1-x}As$ structure at application of reverse voltage to the structure. Because of the proportionality, $t_{\rm dr} \sim v_{\rm dr}^{-1} \sim I_0^{-1}$, the current multiplication coefficient $K = \tau/t_{\rm dr}$ is proportional to the bias current I_0.

The charge collected from the n^--GaAs layer is equal to the charge collected from the $Al_xGa_{1-x}As$ layer $Q_{\rm c}$, multiplied by a factor K:

$$Q_{\rm f} = Q_{\rm c}K. \quad (25)$$

The short-circuit current through the structure is

$$I_{\rm D} = I_0 + I_{\rm X}K, \quad I_{\rm X} = \beta P_{\rm abs}, \quad (26)$$

where $P_{\rm abs}$ is the absorbed X-ray power and β is the current/absorbed power sensitivity. For the structure $Al_xGa_{1-x}As$/GaAs one finds that $\beta = 0.25\eta$ (see Eq. (11)).

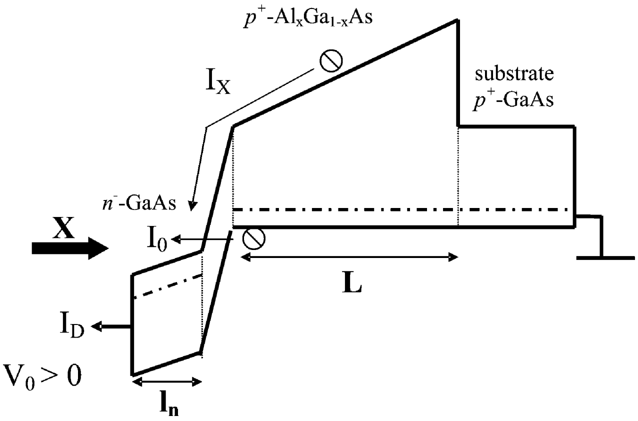

Fig. 11. The schematic band diagram of the n^--GaAs/p^+-Al$_x$-Ga$_{1-x}$As heterostructures with applied reverse voltage. I_X denotes the electron flow in the graded-gap field, I_0 indicates the $p{-}n$ junction reverse current.

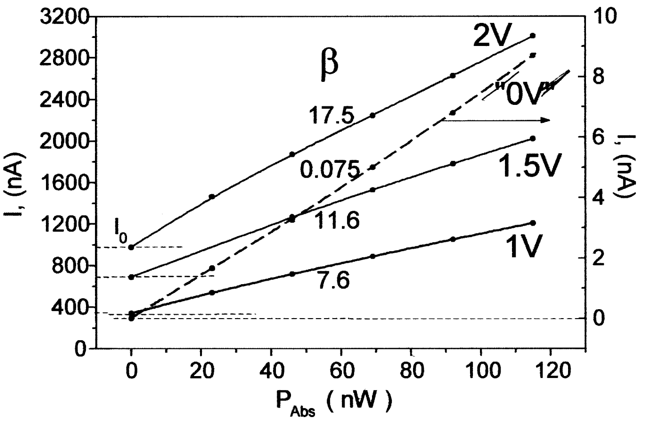

Fig. 12. The short-circuit current I_D through the n^--GaAs/ p^+-Al$_x$Ga$_{1-x}$As heterostructure as a function of absorbed X-ray power at different bias voltages (V) and currents (I_0). The curves are labelled by the current/absorbed power sensitivity. The dashed line corresponds to $I_\mathrm{D}(P_\mathrm{abs})$ without application of any bias (right scale). The dotted lines indicate the levels of bias current I_0 at $P_\mathrm{abs} = 0$.

Figure 12 shows the dependence of the experimentally measured current through the device on the absorbed X-ray power at different bias currents I_0. An X-ray tube with a Cu anode has been used as an X-ray radiation source. The absorption coefficient of this radiation in Al$_x$Ga$_{1-x}$As is $\alpha_\mathrm{X} \approx 400$ cm^{-1}, and 55% of the incident power was absorbed in the Al$_x$Ga$_{1-x}$As layer of thickness $L = 20$ μm. The measured current sensitivity β at the zero bias current ($I_0 = 0$) is equal to $I_\mathrm{X}/P_\mathrm{abs} = 0.075$ A/W. This corresponds to the charge collection efficiency $\eta \approx 0.33$.

The multiplication of the collected charge increases with increasing I_0 and achieves $K = 234$ at $I_0 = 0.97$ μA. Correspondingly, the current/absorbed power sensitivity increases by a factor of 234 and achieves $\beta = 17.5$ A/W. This is 70 times larger than the sensitivity $\beta = 0.25$ A/W in the case of 100% collection of charge generated in Al$_x$Ga$_{1-x}$As. Note that the amplification effect is obtained at applied reverse bias of only a few volts (Fig. 12). Due to the multiplication effect, the novel X-ray radiation detectors are much more sensitive than conventional $p{-}n$ Si or GaAs detectors.

6. Conclusions

1. Al$_x$Ga$_{1-x}$As layers of the thickness up to 100 μm absorb efficiently X-ray power in the range of $E_\mathrm{X} = 3{-}0$ keV, and they can be used as soft X-ray–light converters. Detectors of area 2×3 cm^2 with homogeneous luminescence were fabricated. It is shown experimentally by the direct read-out of the Al$_x$Ga$_{1-x}$As layer X-ray luminescence image by the CCD camera that the contrast and spatial resolution of the image details is better than 15 lines/mm.

2. The volt–watt efficiency β_v increases with decreasing X-ray power. Values of $\beta_v = 1.1{\cdot}10^5$ V/W at $W_\mathrm{X\ abs} = 2{\cdot}10^{-6}$ W and $\beta_v = 5{\cdot}10^5$ V/W at $W_\mathrm{X\ abs} \approx 2{\cdot}10^{-7}$ W are observed with the thin 15 μm Al$_x$Ga$_{1-x}$As layers. A 100% charge collection efficiency is achieved in a 27 μm thick Al$_x$Ga$_{1-x}$As detector without application of any external bias voltage.

3. The charge generated by the ionizing radiation in the p^+-Al$_x$Ga$_{1-x}$As layer is collected by graded-gap field and directed to thin n^--GaAs where it is multiplied. The new charge multiplication method by increasing the $n^-{-}p^+$-heterojunction reverse current is realized. The achieved collected charge multiplication in n-GaAs/p^+-graded-gap Al$_x$Ga$_{1-x}$As structures exceeds 200. The current response β of the new detector is much larger than in conventional Si or GaAs detectors.

4. The new structure can be used as a high efficiency single particle detector (^{241}Am alpha particles) operating without application of any bias.

References

[1] J. Požela, K. Požela, A. Šilėnas, V. Jasutis, L. Dapkus, and V. Jucienė, X-ray luminescence spectra of graded-gap Al$_x$Ga$_{1-x}$As structures, Nucl. Instrum. Methods A **460**, 41–44 (2001).

[2] J. Požela, K. Požela, A. Šilėnas, V. Jucienė, L. Dapkus, V. Jasutis, G. Tamulaitis, A. Žukauskas, and R.-A. Bendorius, The AlGaAs light emitted particle detector, Nucl. Instrum. Methods A **432**, 169–172 (1999).

[3] J. Požela, K. Požela, A. Šilėnas, V. Jasutis, L. Dapkus, and V. Jucienė, The $Al_xGa_{1-x}As$ X-ray imaging detector, Nucl. Instrum. Methods A **460**, 119–122 (2001).

[4] J. Požela, K. Požela, A. Šilėnas, V. Jucienė, L. Dapkus, and V. Jasutis, X-ray luminescence of AlGaAs structure, Lithuanian J. Phys. **39**(2), 139–147 (1999).

[5] A.M. Gurevich, *X-ray Luminofors and Screens* (Atomizdat, Moscow, 1976) [in Russian].

[6] A. Šilėnas, J. Požela, K. Požela, V. Jasutis, L. Dapkus, and V. Jucienė, Non-uniformly-doped graded-gap AlGaAs X-ray detectors with high photovoltaic response, Nucl. Instrum. Methods A **487**, 54–59 (2002).

[7] A. Šilėnas, J. Požela, K. Požela, V. Jasutis, L. Dapkus, and V. Jucienė, Graded-gap AlGaAs X-ray detectors with fast photovoltaic response, Materials Science Forum **384–385**, 287–290 (2002).

[8] A. Šilėnas, K. Požela, L. Dapkus, V. Jasutis, V. Jucienė, J. Požela, and K.M. Smith, Graded-gap $Al_xGa_{1-x}As$ X-ray detector with collected charge multiplication, in: *4th International Workshop on Radiation Imaging Detectors* (Amsterdam, 8–12 September 2002) p. 92.

VARIZONINIO $\mathbf{Al_xGa_{1-x}As}$ JONIZUOJANČIOS SPINDULIUOTĖS JUTIKLIAI

A. Šilėnas

Puslaidininkių fizikos institutas, Vilnius, Lietuva

Santrauka

Pateikti varizoninių $Al_xGa_{1-x}As$ jonizuojančios spinduliuotės jutiklių tyrimai bei jutiklių su optiniu ir elektriniu atsakais veikimo mechanizmai. 2×3 cm^2 ploto jutikliuose pasiektas didelis vidinis Röntgen'o spinduliuotės pavertimo šviesa efektyvumas ir vaizdo erdvinė skyra, geresnė negu 15 linijų/mm. Pagrindinė išorinį efektyvumą mažinanti priežastis yra mažas visiško atspindžio kampas nuo jutiklio paviršiaus. Pasiektas 100% jonizuojančios spinduliuotės generuoto krūvio surinkimas 27 μm storio $Al_xGa_{1-x}As$ sluoksnyje vidiniu varizoniniu lauku, neprijungus jokios išorinės įtampos. Parodyta, kad varizoniniai p-$Al_xGa_{1-x}As$/n-GaAs dariniai be išorinio postūmio gali būti naudojami pavienėms jonizuojančioms dalelėms (^{241}Am alfa dalelės) detektuoti. Realizuotas naujas surinkto krūvio dauginimo metodas p^+-$Al_xGa_{1-x}As$/n-GaAs dariniuose didinant atgalinę $p^+ - n^-$ sandūros srovę. Pasiekta stiprinimo koeficiento vertė viršija du šimtus, o jutiklio srovės jautris padidėja iki 17,5 A/W ir gerokai viršija įprastinių puslaidininkinių Si ir GaAs jutiklių jautrį.